

---

# MULTI-VIEWPOINT AND MULTI-EVALUATION WITH FELICITOUS INDUCTIVE BIAS BOOST MACHINE ABSTRACT REASONING ABILITY

---

**Qinglai Wei**

State Key Laboratory for Management and Control of Complex Systems,  
Institute of Automation, Chinese Academy of Sciences  
School of Artificial Intelligence, University of Chinese Academy of Sciences  
Beijing, China  
qinglai.wei@ia.ac.cn

**Diancheng Chen**

State Key Laboratory for Management and Control of Complex Systems,  
Institute of Automation, Chinese Academy of Sciences  
School of Artificial Intelligence, University of Chinese Academy of Sciences  
Beijing, China  
chendiancheng2020@ia.ac.cn

**Beiming Yuan**

School of Artificial Intelligence, University of Chinese Academy of Sciences  
Beijing, China  
yuanbeiming20@mailsucas.ac.cn

October 28, 2022

1 2

**ABSTRACT**

Great endeavors have been made to study AI's ability in abstract reasoning, along with which different versions of RAVEN's progressive matrices (RPM) are proposed as benchmarks. Previous works give inkling that without sophisticated design or extra meta-data containing semantic information, neural networks may still be indecisive in making decisions regarding RPM problems, after relentless training. Evidenced by thorough experiments and ablation studies, we showcase that end-to-end neural networks embodied with felicitous inductive bias, intentionally design or serendipitously match, can solve RPM problems elegantly, without the augment of any extra meta-data or preferences of any specific backbone. Our work also reveals that multi-viewpoint with multi-evaluation is a key learning strategy for successful reasoning. Finally, potential explanations for the failure of connectionist models in generalization are provided. We hope that these results will serve as inspections of AI's ability beyond perception and toward abstract reasoning. Source code can be found in <https://github.com/QinglaiWei/CASIA/RavenSolver>.

**Keywords** Abstract Reasoning, Raven's Progressive Matrices, Inductive Bias, Convolutional Neural Network, Transformer, Generalization

---

<sup>1</sup>All authors contributed equally to this work.

<sup>2</sup>Corresponding Author: Diancheng Chen (chendiancheng2020@ia.ac.cn)

## 1 Introduction

From expert system with elaborated designed rules to the renaissance of neural network, AI practitioners never ceased to work on machine intelligence to make it a counterpart of human intelligence. The tremendous success of machine learning in areas like visual perception [1, 2, 3], natural language processing [4, 5, 6], or generative models [7, 8, 9], intrigues researchers to study the reasoning ability of AI. Representative works cover, but not limit to, visual question answering [10, 11], flexible application of language models [12, 13, 14], and abstract reasoning problems [15, 16]. Here we consider the RPM problem, originally developed for the purpose of IQ test [17], and recently serve as a benchmark for the evaluation of AI’s abstract reasoning ability.

Without loss of generality, RPM problem is formalized within three steps. First, sample rules from a predefined rule set, which consists of changing modes of visual attributes. Second, design attribute values to be in consistency with the sampled rules. Some visual attributes may play the role of distracter, meaning that their values will change randomly. Finally, render images basing on the generated information. Instantiated RPM problem is composed of a context and an answer pool: the context is a  $3 \times 3$  image matrix, with image in the lower right corner missing. While the answer pool contains 8 images for selection. Test-taker is required to select one most fitted image from the answer pool to complete the matrix, so as to make it compatible with the internal rules.

To achieve satisfying reasoning accuracy in RPM problems, it is expected that models should be able to extract visual attributes, distinguish between attributes related to downstream tasks and the irrelevant ones, in the meantime infer about the underlying rules. Combined together, tackling abstract reasoning problems requires one more step forward than perception, namely the extra reasoning part.

In this work, we solve RPM problems in an end-to-end manner. Three key points to follow when developing the black-box RPM solver: distinct modularization to imitate the whole reasoning process, encapsulation of two potential RPM characteristics, namely permutation-invariance and transpose-invariance, into the inductive bias design of the model architecture, and the implementation of multi-viewpoint and multi-evaluation strategy. To be specific, distinct modularization requires both the cooperation and a clear boundary between the feature extraction module and the reasoning module, which requires that each module attends to its own duty properly, otherwise adding a reasoning module is nothing but merely extending the depth of a neural network. This issue is addressed by injecting available inductive bias to the reasoning module to make it aware of the permutation-invariance and transpose-invariance characteristics of RPM problems. Finally, in light of that in RPM problems, various visual attributes and rules are involved, resulting in abundant attribute-rule combinations, we equip the feature extraction module with multi-viewpoints strategy and the reasoning module with multi-evaluation strategy, which endows with the ability of attending to RPM problem in different perspectives at the same time to the neural RPM solver.

The results of our work are promising and intriguing in several ways. First, it shows that either models based on convolutional neural networks (CNN) or vision transformer (ViT [18]) produces competitive reasoning accuracies, which overturns some stereotypes, like the incompetence of elementary visual models in solving RPM problems, or extra meta-data is necessary for attaining better results [19, 20]. Second, it is hypothesized with experimental proofs that unexpected rule summarization pattern is to blame for unsatisfying generalization results.

## 2 Related Work

In this section we introduce two RPM datasets, namely RAVEN[19] and PGM[20], and several neural networks for solving them.

### 2.1 RPM Dataset

Both RAVEN and PGM follow the general construction guideline described before, but they differ in many ways. RAVEN consists of 7 distinct configurations with different difficulty levels. The easiest configuration is ‘Center’, in which each panel of the problem matrix only has one entity, while harder configurations such as ‘ $3 \times 3$  Grid’ has at most nine entities in each panel. Test-takers are required to observe the changing patterns row-wise, extract visual attributes, summarize rules controlling the flow of pattern changes, then make choice to complete the problem matrix. The most difficult configuration, ‘O-IG’, requires test-takers to divide entities in each panel into two groups, each of which follows one set of rules, then perform reasoning respectively. While each panel of the PGM problem matrix may have entities in the foreground and lines in the background. Test-takers are expected to observe the changing pattern row-wise and column-wise simultaneously, summarize the potential rules in foreground and background respectively, and then complete the reasoning task accordingly.

Statistically, RAVEN has 6.29 rules per question in average, compared to 1.37 in PGM [19]. RAVEN has two fixed visual attributes as distracters, while PGM is way more flexible in that any visual attribute can be an distracter. RAVEN has its rules encoded row-wise, while one must check row-wise and column-wise simultaneously for summarizing rules in PGM. By the way, PGM also has different configurations, for the generalization analysis purpose, which means different versions of distribution shift between the training set and the test set are designed in PGM.

## 2.2 RPM solvers

literatures of RPM solver expand rapidly in recent years. Here we roughly divide them into three categories. The first one is end-to-end black-box RPM neural solvers, accounting for the majority of previous works. The second one leverages symbolic AI in order to obtain results beyond reasoning accuracies, such as model interpretability. The third one’s interests focus on studying the validity of datasets.

The end-to-end black-box models focus on improving the reasoning accuracy on RPM problems. The developers of both RAVEN and PGM dataset conclude that prevalent visual models fail to solve RPM problems, and adding extra labels containing information of structure or rule do improve the results to some extent [19, 20]. After that, in LEN[21], researchers argue that the main challenging in solving RPM problems is the elimination of distracting information. CoPINet [22] and DCNet [23] are proposed to leverage contrastive learning in reasoning. MRNet [24] shows that fusing information of RPM images processed by different CNN blocks connected serially do help the model to capture multiple visual attributes simultaneously, it is also the first work to report that extra meta-data may do harm to the network performance to some extent. In SCL [25], tensor scattering is performed to make each scattered part attend to specific visual attributes or rules. SAVIR-T [26] extracts intra-image information and inter-image relations so as to facilitate reasoning ability. Researchers also find that potential semantically disentangled visual features leads to better reasoning performances [27].

Symbolic AI powered methods bring forth higher reasoning accuracies and stronger model interpretability. In PrAE [28], a neural symbolic system performs probabilistic abduction and execution to generate an answer image, with the prior knowledge of rules. While ALANS [29] manages to get rid of prior rule knowledge and outperforms monolithic end-to-end model in terms of generalization ability. NVSA [30] uses holographic vectorized representations and ground-truth attribute values to build a neural-symbolic model.

Literatures also show that the answer generation process of RAVEN encourages neural solvers to find shortcut solutions instead of discovering rules [31, 24]. Dataset like I-RAVEN and RAVEN-Fair with refining answer generation strategies are proposed to address this issue [31, 24].

## 3 Method

We propose RPM solvers in two forms, RS-CNN and RS-TRAN, which are composed of convolutional neural network and transformer blocks respectively. We show that RS-CNN can perform accurate reasoning with proper inductive bias design, while the inductive bias of RS-TRAN naturally lends itself to RPM problems without extra design, and that multi-viewpoint with multi-evaluation mechanism is able to improve the reasoning ability of RS-TRAN remarkably. We will firstly introduce each network architecture for solving RAVEN, then discuss the necessary modifications for applying these models in solving PGM.

### 3.1 RS-CNN

RS-CNN consists of perception module and reasoning module. The perception module is expected to capture various visual features simultaneously. We follow the architecture of multi-scale encoder of MRNet[24], with different convolutional blocks attending to different visual attributes, as shown in Fig. 1.

Fig. 2 depicts the reasoning module, which constitutes the above-mentioned downstream task. For each block of the perception module ( $E_H$ ,  $E_M$ , and  $E_L$ ), we concatenate the features of images in the problem matrix row-wise, then feed each concatenated features into an information fusion module (IFM) formed by convolutional blocks to obtain the row-wise aggregated features. Note that rules can only be determined after observing at least two rows of the problem matrix, as a result of that, every two rows of aggregated information are paired up and fed into rule extraction module (REM) formed by bottleneck residual convolutional blocks to obtain the rule representation, which comes from one perspective of the perception module. Finally, we concatenate the rules derived by each block of the perception module to be the final rule representation.

The network architecture introduced so far covers all the basic elements for constructing CNN based solver. Apart from the perception module, the aggregated information and observing two rows simultaneously for rule extraction resembles

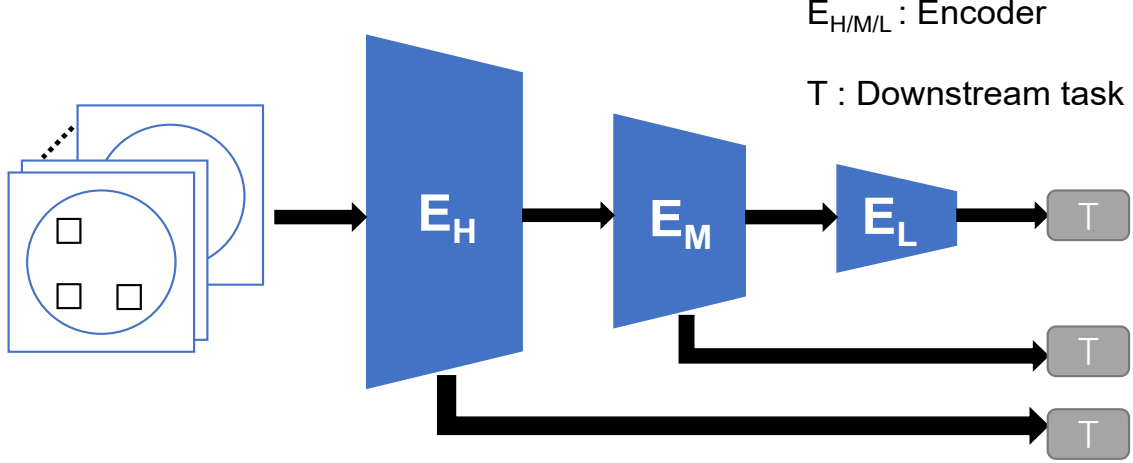


Figure 1: Simple illustration of multi-scale encoder developed in MRNet.  $E_H$ ,  $E_M$ , and  $E_L$ , connected serially, are residual convolutional blocks with decreasing kernel size. Not only the information processed by a former block will flow into the successor block, but also the output of each block will serve as features for downstream tasks individually.

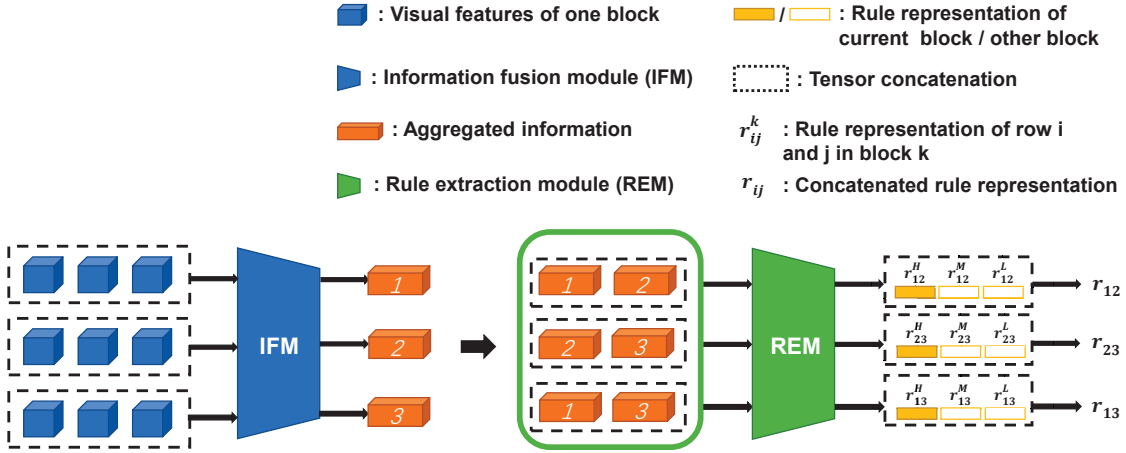


Figure 2: Simple illustration of the reasoning module of RS-CNN. The reasoning module takes the features produced by each block of the perception module individually, and generates aggregated row information of the problem matrix by IFM, then summarizes potential rules for each pair of aggregated row information by REM, and finally concatenates the summarized rules of each block, in the order of  $E_H$ ,  $E_M$ , and  $E_L$ .

triplets in relation module of MRNet and shared rule extraction mechanism in SAVIR-T, and can be deemed as a combination of these two models. To be specific, RS-CNN continues to use the multi-scale encoder architecture and the relation module in MRNet, merge information from each encoder after proper reasoning like MRNet, while substitute the sophisticated pattern module in MRNet with vanilla residual convolutional blocks. Meanwhile, the resemblance between RS-CNN and SAVIR-T lies in the fact that both of them observe two rows simultaneously to obtain a rule representation, and this operation is natural since it is the only way to eliminate ambiguous rule representation.

We wrap up the discussion of RS-CNN for RAVEN by introducing the inductive bias design, which conveys the property of permutation-invariance. Permutation-invariance indicates that exchanging the order of any two rows of the problem matrix does not effect the internal rules [33]. Previous works also devoted themselves to design neural networks which live up to permutation-invariance criterion [22, 24, 26]. Here we follow the spirit of modularization and endow the reasoning module with permutation-invariance property since rules should be invariant after row-wise permutation in RAVEN. As shown in Fig. 3(a), we explicitly model the aggregated information and the permuted ones, and feed them into the REM module. During training phase, we set four rule representations as guiding representations, which are  $r_{12}$ ,  $r_{21}$ ,  $r_{a1}$ ,  $r_{a2}$ , and compare each of them with two rule representation sets:  $\{r_{1c}\}_{c=1}^8$ ,  $\{r_{2c}\}_{c=1}^8$ , respectively, in terms of cosine similarity, as shown in Fig. 3(b). The training goal is to close the gap between the guiding representations

and  $r_{1c}, r_{2c}$  with the right answer (that is  $r_{1a}, r_{2a}$ ), while drift the guiding representations away from  $r_{1c}$  and  $r_{2c}$  with wrong answers. We borrow the idea from contrastive learning [34], and consider each guiding representation as an independent query, and  $\{r_{1c}\}_{c=1}^8, \{r_{2c}\}_{c=1}^8$  as two dictionaries, where the correct answer and wrong answers are treated as positive and negative samples. Each query and dictionary is paired up to compute an InfoNCE [35, 36] loss, which leads to eight symmetric and independent losses. In this setting, InfoNCE loss is CrossEntropy loss augmented with temperature as a hyperparameter. During test phase, the guiding representations reduce to  $r_{12}, r_{21}$ , since the index of right answer is unknown. SAVIR-T is also trained by comparing rule representation, as a matter of fact, the loss function in RS-CNN is a bigger, more flexible version of what is adopted in SAVIR-T, with more rule representations available for comparison, and InfoNCE loss.

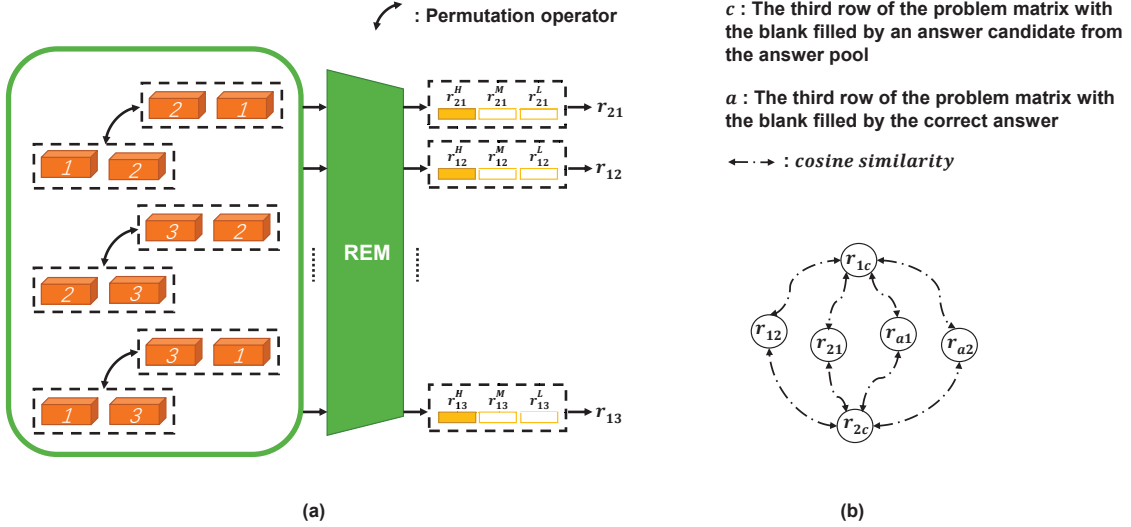


Figure 3: (a) Illustration of the method of endowing RS-CNN with permutation invariance property. Aggregated information and the corresponding permuted ones are modeled explicitly and send to REM to obtain rule representations, and each aggregated information with its permuted pair are expected to output same rule representations. (b) Compute cosine similarity score between the guiding representations and two sets of rule representations  $\{r_{1c}\}_{c=1}^8, \{r_{2c}\}_{c=1}^8$ .

We introduce the necessary revisions for adapting RS-CNN to PGM dataset. We firstly assume that in PGM, both row-wise and column-wise rules always exist (which is not true). As shown in Fig. 4, to make RS-CNN support PGM, we apply the REM module to every problem matrix which is preprocessed by IFM module row-wise and column-wise simultaneously, then pair up each row rule representation with the column one by concatenation to obtain a bunch of row-column rule representations, with the consideration of permutation invariance. Then we designate guiding representations, who enjoy the intended rule representation of the problem matrix. These guiding representations are treated as queries. Next, rule representation with the information from the third row / column are clustered into four groups. Each group of rule representation is treated as a dictionary, within which every answer from the answer pool is considered. Note that there is no intersection between queries and dictionaries. The neural network is optimized to align each query with members in each dictionary which are blessed with the right answer and drift away from others. Further more, notice that transpose the problem matrix, which is equivalent to change the concatenation order of row-column representation, shall not effect the answer.

However, the fact is, PGM is designed such that both rows and columns are allowed to change randomly, as long as there exists at least one rule. The aforementioned design is not compatible with PGM because it tries to align every ‘random change’ representation with each other. Efforts has been made to identify the ‘random change’ pattern by an extra neural network and proves futile. In practice, the row-column rule representation is further processed with a shallow MLP layer, which is effective in mitigating the negative influence of aligning the ‘random change’ representations.

To sum up, the idea of explicitly design of transpose and permutation invariance as inductive bias in RS-CNN has pros and cons. First, implement these inductive bias in the reasoning module rather than shuffle the problem matrix directly saves computational resources by skipping repetitive computation in the perception module. Second, the whole process mimics the reasoning procedures of human. However, although the idea behind RS-CNN is compatible with RAVEN, it has conflicts with PGM, which can only be alleviated to some extent. The drive to solve PGM and RAVEN completely and elegantly gives birth to RS-TRAN.

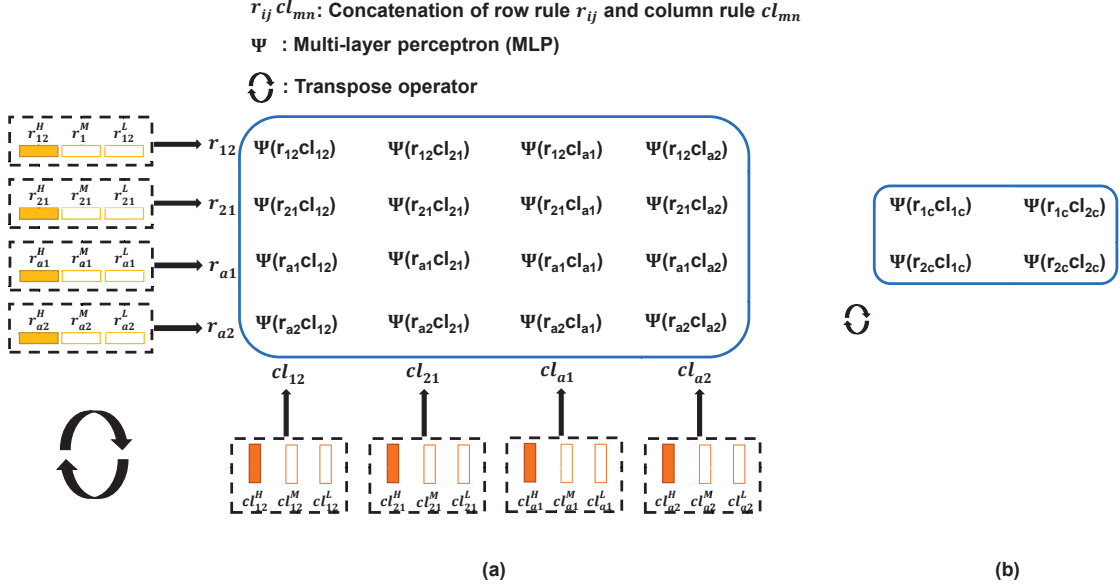


Figure 4: Illustration of revisions for applying RS-CNN to PGM dataset. Concatenate each row rule representation with column rule representation, then obtain each row-column rule representation by feeding the concatenated vector to a two layer MLP. (a) List of row-column rule representations which are designated as guiding representations (queries), with the consideration of permutation invariance. (b) Four sets of row-column rule representations(dictionaries), where each answer candidate in the answer pool is involved. Note that both two concatenation orders (row-column and column-row) should be considered to live up with transpose invariance criterion.

### 3.2 RS-TRAN

The top-3 successful end-to-end RPM solvers up-to-date in terms of reasoning accuracy (MRNet, SAVIR-T, SCL) have one thing in common: trying to encode image features in different perspectives. Specifically, MRNet adopts multi-scale encoders, SAVIR-T combines residual convolutional block with Transformer block to produce multiple visual tokens, while SCL scatters extracted visual representations into pieces. The present RS-TRAN follows the spirit of these methods, with a more scalable implementation.

The perception module of RS-TRAN is developed with the backbone of ViT and the implementation of multi-viewpoint mechanism. As shown in Fig. 5, each image in the problem matrix and the answer pool is first split into 16 patches and then fed into a linear embedding layer with positional encoding, whose output will be sent to Transformer blocks. In the output side of the last Transformer block, between using global averaging pooling and special classification token [5, 18], we choose neither of them and leave all the outputs unprocessed, and end up with multiple outputs for each image. Such move can be interpreted as maintaining the diversity of the global features in the perspective of every patch, and the realization of multi-viewpoint mechanism.

In the reasoning module of RS-TRAN, we process feature representations of each viewpoint individually. when dealing with RAVEN dataset, for every perspective, set the problem matrix with the right answer or wrong answer plugged in as positive and negative sample. As shown in Fig. 6, representations are concatenated row-wise to produce three aggregated information, which will be sent to Transformer blocks after a bottleneck module and positional encoding. Similar to the perception module, the outputs of the last transformer block will be left unprocessed, and each of which will be sent to a scoring module formed by bottleneck MLP layers to obtain a score. That means the amount of score for each problem matrix equals the product of number of outputs in the perception module and number of outputs in the reasoning module. All scores are averaged to produce the final score. Setting CrossEntropy loss as the loss function, the network is optimized so that the score of the problem matrix with the right answer outnumbers others.

The necessary revisions for adapting RS-TRAN to PGM dataset is way more straightforward than RS-CNN. Fig. 7 shows how to process one viewpoint of feature representations in the reasoning module. Intuitively, PGM needs both aggregated row and column information to complete the reasoning process. All the aggregated information is sent to the Transformer blocks, while other operations remain the same as applying RS-TRAN to solve RAVEN.

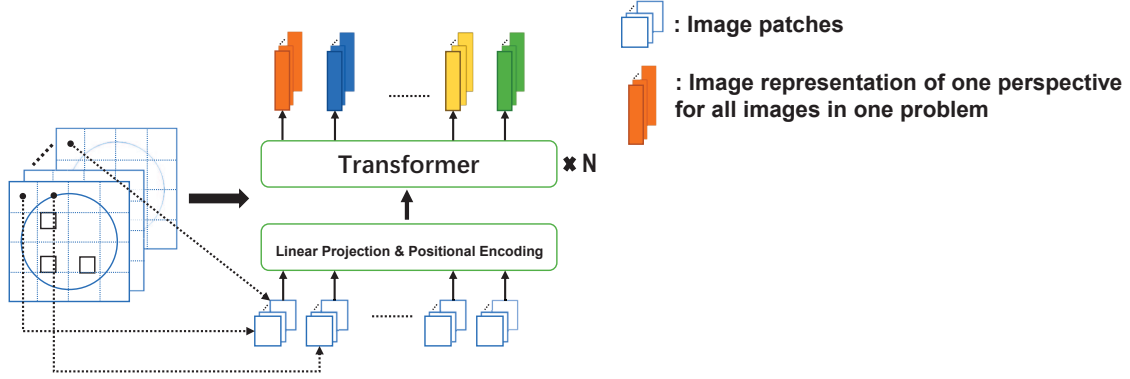


Figure 5: Illustration of the perception module in RS-TRAN. Each image in the problem matrix is processed independently: split into patches, processed by the same linear embedding layer with positional encoding, then several Transformer blocks. The output of each image will be a bunch of feature representations, each of which stands for one viewpoint. We collect the feature representation of all the images in the problem matrix viewpoint by viewpoint.

The explicit implementation of permutation invariance or transpose invariance in RS-TRAN is not necessary: changing the order of aggregated information is equivalent to the capability of permutation or transpose operator, and in RS-TRAN, it can be shown that the order of the aggregated information only influences the order of output scores (leave alone the effect of positional encoding), which is of no effect after the averaging operation. In this scenario, learnable positional encoding [37] is preferred since the fixed version may break the compatibility between the model and the inductive bias.

RS-TRAN bears a resemblance to RS-CNN in that both of them consist of perception module and reasoning module, while RS-TRAN alone ends up with a scoring module. Apart from the most superficial distinction that RS-CNN is made of CNN blocks while RS-TRAN is made of ViT and transformer blocks, RS-TRAN is also different from RS-CNN in three other ways. The first difference is implicit implementation of permutation invariance and transpose invariance, which leads to a refreshing and uncomplicated network architecture. The second difference is that each problem will be observed and evaluated multiple times in RS-TRAN, indicating that the diversity endowed by the ‘multiple outputs’ architecture of transformer will be maintained till the last. The third difference is that, RS-TRAN produces a score for every problem matrix to be evaluated, instead of explicit comparison between rule representations.

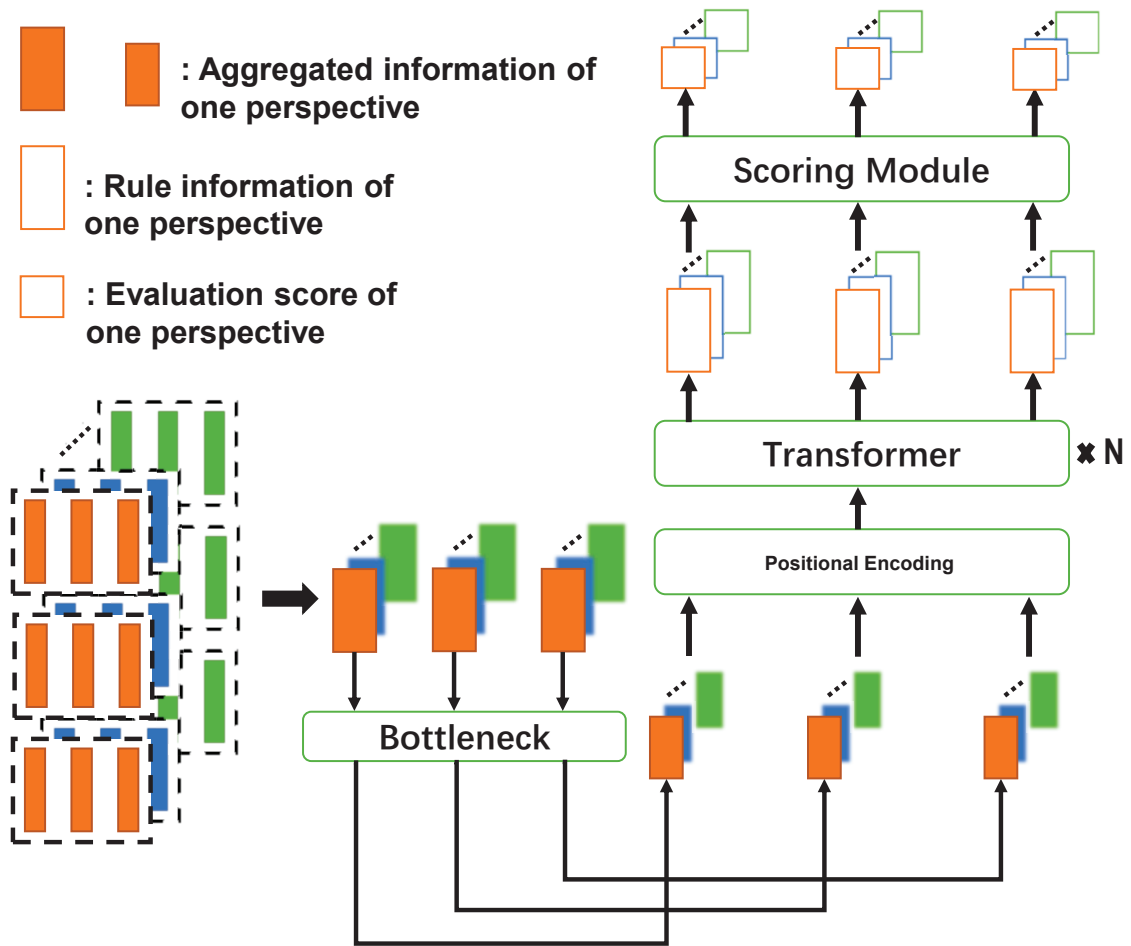


Figure 6: Illustration of the reasoning module in RS-TRAN. In each viewpoint, each problem matrix with an answer candidate is evaluated multiple times. The bottleneck module is introduced to adjust the dimension of the aggregated information and replace the linear embedding layer.



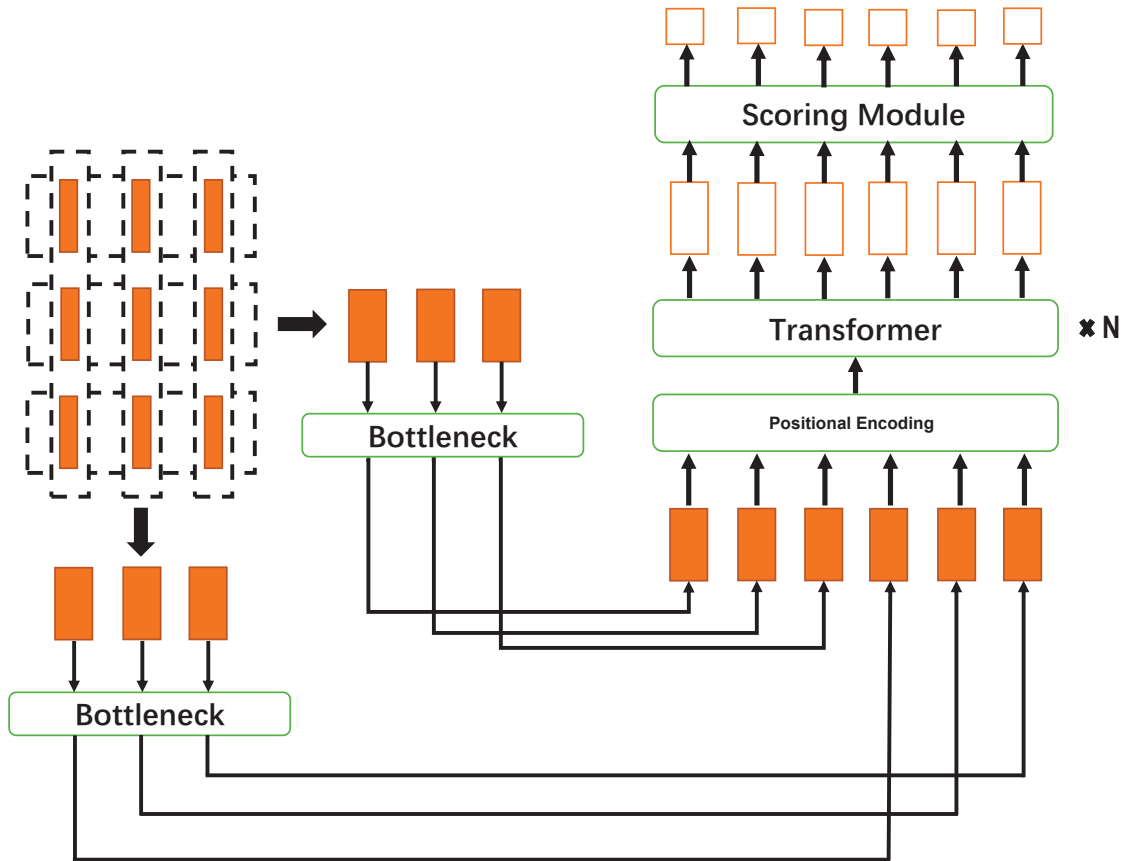


Figure 7: Illustration of revisions for applying RS-TRAN to PGM dataset. For simplicity, only one viewpoint of the image representations is shown. The modification we made here is to obtain column aggregated information, and then blend it with the row aggregated information.

## 4 Experiments

In this section, we report the reasoning accuracy of the proposed models in RPM problems, compare these results with former state-of-the-arts: WReN [20], LEN, CoPINet, DCNet, SCL, SAVIR-T, MRNet, and SRAN [31]. And then, we evaluate the effect of dataset size, conduct ablation studies to demonstrate the necessity of the proposed network architectures, perform masking experiments to test the validity of multi-viewpoint and multi-evaluation mechanism, and study the generalization ability of the proposed models. The architecture detail of each proposed model and some experimental results are documented in the appendix.

### 4.1 Reasoning Accuracy

For each configuration in RAVEN and I-RAVEN, data is split into training set, validation set and test set, with the size of 80K / 20K / 40K for RS-CNN and 155K / 0.5K / 40K for RS-TRAN. The training session is terminated when the reasoning accuracy of the validation set ceases to improve substantially in the long run, and we report the reasoning accuracy in the test set. Both RS-CNN and RS-TRAN are implemented in Pytorch[38], and optimized by ADAM[39]. The reasoning result is shown in Fig. 8, both the proposed RS-CNN and RS-TRAN shows competitive results in general.

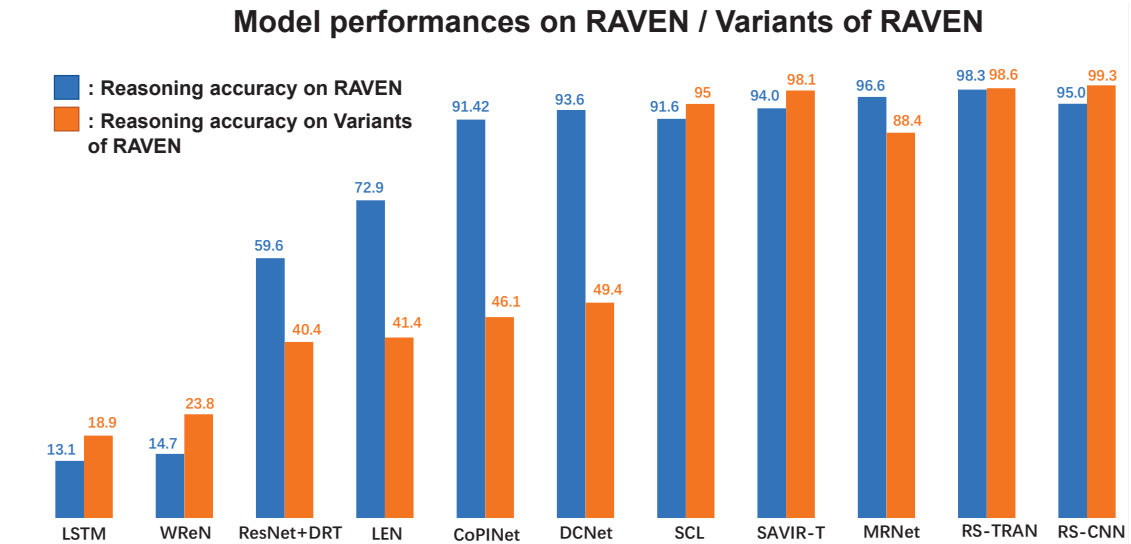


Figure 8: Reasoning accuracies of different models on RAVEN and variants of RAVEN(I-RAVEN or RAVEN-FAIR).

The experiment settings of RS-CNN and RS-TRAN on PGM is on the same page with that of RAVEN, except that the size of training set, validation set and test set is 1200K / 20K / 400K. As shown in Fig. 9, RS-TRAN surpasses the former SOTA results reported in SCL, SVAIR-T, and MRNet, while RS-CNN achieves the reasoning accuracy of 82.8%.

The success of RS-CNN and RS-TRAN, along with the failure of RS-CNN in PGM dataset, confirms our hypotheses: the choice of backbone network does not matter, as long as the architecture inductive bias agrees with the characteristics of the RPM problems.

### 4.2 Effect of dataset size

We also investigate the impact of the dataset size in RS-CNN and RS-TRAN. The performance of traditional neural networks depends on the size of dataset heavily[40], so is the case with Transformer-related networks [41, 18]. For simplicity, we only take ‘Center’, ‘Distribute 9’ and ‘O-IG’ in RAVEN and I-RAVEN for example.

First, notice that the test accuracy of RS-CNN in RAVEN is mediocre compared with its results in I-RAVEN, so we increase the size of training set in RAVEN to 155K/configuration. Second, viewing that RS-TRAN requires tons of data in the experiment settings, so we decrease the training set size of I-RAVEN to 80K/configuration.

The general conclusion is not surprising: as shown in Table 1, bigger dataset size leads to better performance. Specifically, RS-CNN improves dramatically when the size of training set increases from 80K to 155K, while RS-

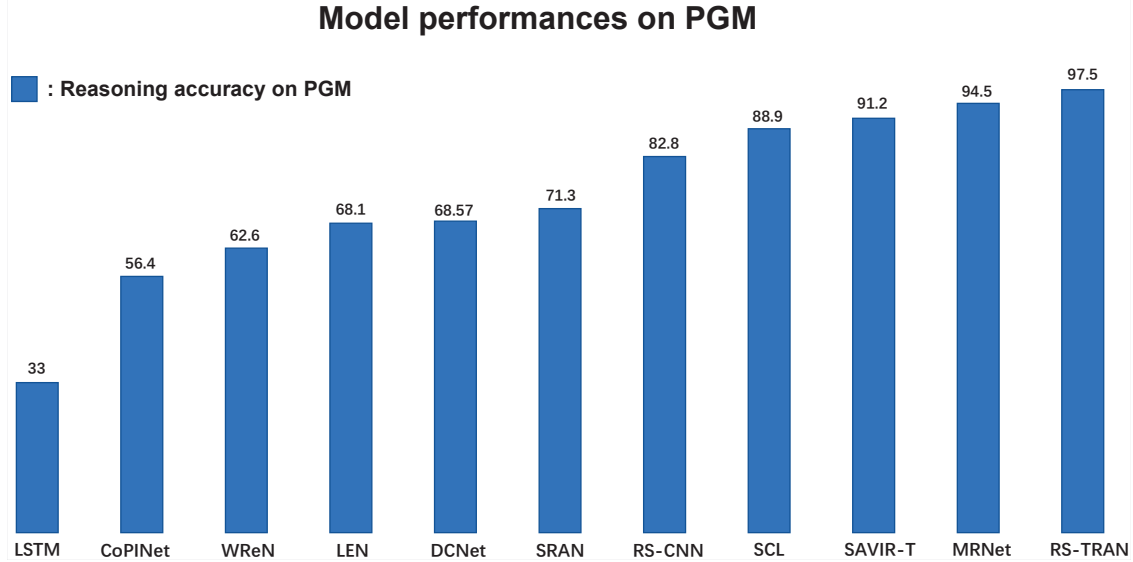


Figure 9: Reasoning accuracies of different models on PGM.

Table 1: Effect of dataset size on RS-CNN and RS-TRAN.

Model	Test Accuracy(%) of RAVEN/I-RAVEN		
	Center	3 × 3 Grid	O-IG
RS-CNN(80K)	100/-	84.5/-	87.6/-
RS-CNN(155K)	100/-	94.2/-	99.2/-
RS-TRAN(80K)	-/99.6	-/90.1	-/93.7
RS-TRAN(155K)	-/99.8	-/94.0	-/95.1

TRANS already has good performance when the dataset size is 80K, and the results can be further improved by expanding the training dataset size.

### 4.3 Ablation Studies

In this part, we dive deeper into the architecture of RS-CNN and RS-TRAN, discuss the necessity of injecting inductive bias into RS-CNN, and the plausibility of RS-TRAN on the ‘natural expressiveness’ of these inductive biases. We also study the effectiveness of multi-viewpoint and multi-evaluation of RS-TRAN. All the ablation studies are conducted on PGM, and ‘Center’, ‘Distribute 9’ and ‘O-IG’ configurations of I-RAVEN.

Table 2: Effect of inductive bias on RS-CNN and RS-TRAN.

Model	Test Accuracy(%) of I-RAVEN and PGM			
	Center	3 × 3 Grid	O-IG	PGM
RS-CNN	100	97.9	99.2	82.8
RS-CNN(Plain)	100	74.7	75.7	76.1
RS-TRAN	99.9	94.6	96.6	97.5
RS-TRAN(Aug)	99.0	94.6	97.1	96.1

In RS-CNN, not taking permutation and transpose invariance into consideration means the elimination of all permuted aggregated information in RAVEN and PGM, and the prohibition of transpose operation in PGM. In RS-TRAN, taking permutation and transpose invariance into consideration means the explicit traversal of input ordering for the reasoning module. Let RS-CNN(Plain) refers to RS-CNN without the consideration of permutation and transpose invariance,

while RS-TRAN(Aug) refers to RS-TRAN with explicit augmentation of permutation and transpose invariance. The results of Table 2 conveys strong signals: explicit inductive design is crucial in RS-CNN, while the architecture of RS-TRAN naturally enjoys the property of permutation and transpose invariance, however explicit inductive bias design will do no harm to the performance.

In the other hand, RS-TRAN without the mechanism of multi-viewpoint and multi-evaluation only has a single, averaged output in both the perception module and the reasoning module (denoted as RS-TRAN(Single)). Table 3 tells us that the reasoning accuracy of RS-TRAN will drop sharply in such a situation. The effectiveness of multi-viewpoint and multi-evaluation mechanism is then self-evident.

Table 3: Effect of multi-viewpoint and multi-evaluation on RS-TRAN.

Model	Test Accuracy(%) of I-RAVEN and PGM			
	Center	3 × 3 Grid	O-IG	PGM
RS-TRAN	99.8	94.0	95.9	97.5
RS-TRAN(Single)	99.6	84.1	77.2	68.7

#### 4.4 More on multi-viewpoint and multi-evaluation

Both the reasoning accuracy and the ablation study show the necessity of adopting multi-viewpoint with multi-evaluation mechanism in RS-TRAN, however the detailed effects of this mechanism is still opaque. To have a clearer understanding of it, we design mask experiments to uncover this mechanism.

In RS-TRAN, multi-viewpoint mechanism is implemented by retaining all the outputs of the perception module. Each image of the problem matrix is divided into 16 patches, which leads to 16 viewpoints (outputs) in the perception module. functionality of each output can be roughly probed by masking it out and testing the reasoning accuracy in terms of each specific rule. The same procedures are applicable to multi-evaluation mechanism, too.

For simplicity, we only study the multi-viewpoint mechanism on single-rule data from PGM and ‘3 × 3 Grid’ configuration from I-RAVEN, by masking out half of the outputs in the perception module of RS-TRAN. As shown in Fig. 10, the functionality of the first 8 viewpoints differ greatly from the rear 8 viewpoints. In ‘3 × 3 Grid’ configuration, compared with masking out the front 8 viewpoints, masking out the rear 8 viewpoints deteriorates the reasoning accuracy in a more severe way. While in PGM, the front 8 viewpoints and the rear 8 viewpoints tend to focus on different rules. With the masking technique, the model acquires certain level of post-hoc interpretability [42, 43]. And we conclude that the multi-viewpoint with multi-evaluation mechanism endows the model with the ability of solving problems in several perspectives simultaneously.

#### 4.5 On Generalization

Specifically in PGM, apart from the ‘neutral’ dataset, where the data from the training set and test set is independent and identically distributed (I.I.D.), there are other datasets whose distribution of training sets and test sets are different (Out of distribution, O.O.D.). We evaluate the generalization ability of the RS-TRAN model by training on these datasets. The experiment setting remains the same with the ‘neutral’ case.

Table 4: Generalization Results of RS-TRAN in PGM.

Dataset	Accuracy(%)
Interpolation	77.2
Extrapolation	19.2
Held-out Attribute shape-colour	12.9
Held-out Attribute line-type	24.7
Held-out Triples	22.2
Held-out Pairs of Triples	43.6
Held-out Attribute Pairs	28.4

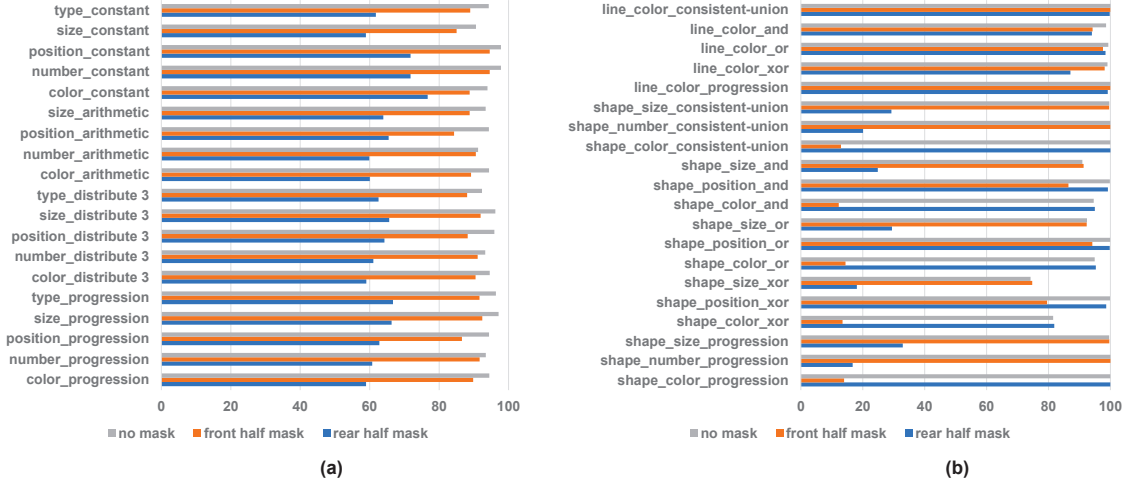


Figure 10: Results of mask experiments. (a) Mask experiments on ‘3 × 3 Grid’ configuration of RAVEN. Data will be collected with respect to each specific rule, e.g., ‘type\_constant’ contains all the image matrices whose rule of ‘type’ are constant. Note that each problem matrix of RAVEN has many rules, by clustering problem matrix with one same rule does not guarantee that all rules each problem matrix have are the same. (b) Mask experiments on single-rule data of PGM. Only problems with one rule will be considered so that no ambiguity will occur.

The results of Table. 4 declare the vulnerability of RS-TRAN facing generalization problems. RS-TRAN achieves 77.2% in the ‘Interpolation’ case, which is a SOTA result, to the best of our knowledge. However, facing dataset with sophisticated compositional structures, well-designed rules and no trace of noise in pixel-level, attempts without remarkably high reasoning accuracies should be deemed as a failure.

Here, in the perspective of RS-CNN, we provide potential explanations for the fail attempts in generalization problems. Recall that RS-CNN evaluates the cosine similarity between the rule representations. Following this logic, it is assumed that rule representations for the same rule, through out the whole dataset, should be identically the same, at least bear extremely close resemblance to each other. However that is not about to happen in end-to-end neural networks. Take the configuration of ‘Center’ and ‘Distribute 9’ in RAVEN for example, 20 image matrices with identical rules are generated for each configuration. As shown in Fig. 11, for each configuration, although rules for these 20 image matrices are identical, perfect match of rule representations can only be observed in the intra-problem situation. That is, RS-CNN does not summarize rules in the way predefined in the dataset, it summarizes rules own its own way and complete the reasoning task, which means it fails in fulfilling the prerequisites for solving problems generalized in the sense of the predefined rules.

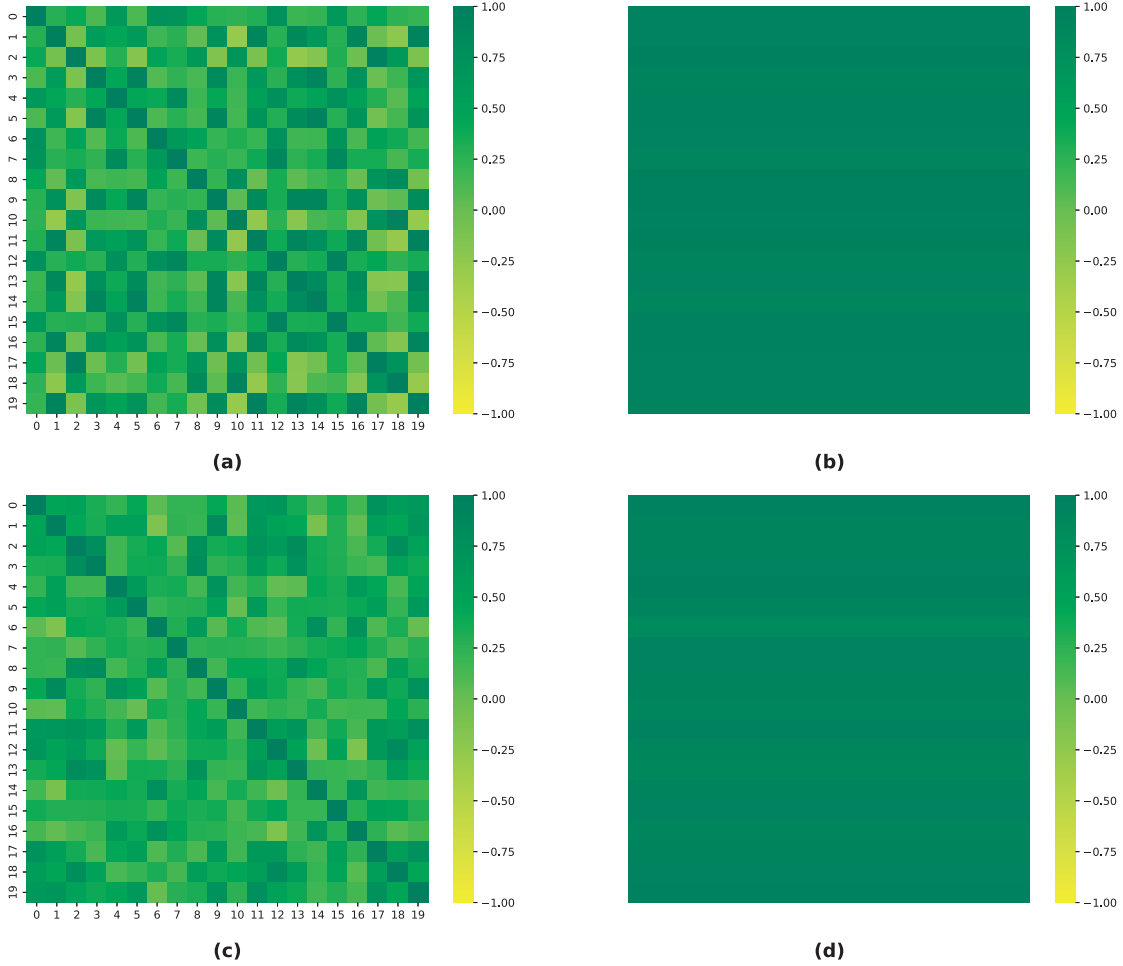


Figure 11: Heat map for rule representation similarity. (a) Inter-problem rule representation similarity for ‘Center’ configuration. (b) Intra-problem rule representation similarity for ‘Center’ configuration. (c) Inter-problem rule representation similarity for ‘Distribute 9’ configuration. (d) Intra-problem rule representation similarity for ‘Distribute 9’ configuration.

## 5 Conclusion

In this paper, we develop two RPM solvers based on CNN and ViT, showing in experiment level that well-designed inductive bias with data compatibility is the key to successful end-to-end RPM neural solvers. Our work also reveals that, meta-data containing non-pixel level information (e.g. rule information, structure information) is not a ‘must-have’ in abstract reasoning, giving that sufficient pixel-level data with full coverage of rules is provided. We also provide hypothesis for the failure of RPM neural solver in generalization problems.

## References

- [1] Deng, J., Dong, W., Socher, R., Li, L. J., Li, K., & Fei-Fei, L. Imagenet: A large-scale hierarchical image database. In IEEE Conference on Computer Vision and Pattern Recognition, 246-255 (2009).
- [2] Krizhevsky, A., Sutskever, I., & Hinton, G. E. Imagenet classification with deep convolutional neural networks. Communications of the ACM, 60(6), 84-90 (2017).
- [3] He, K., Zhang, X., Ren, S., & Sun, J. Deep Residual Learning for Image Recognition. In IEEE Conference on Computer Vision and Pattern Recognition, 770-778 (2016).
- [4] Vaswani, A. *et al.* Attention is All You Need. In Advances in Neural Information Processing Systems, (2017).

- [5] Devlin, J., Chang, M. W., Lee, K., & Toutanova, K. Bert: Pre-training of Deep Bidirectional Transformers for Language Understanding. Preprint at <https://arxiv.org/abs/1810.04805> (2018).
- [6] Brown, T. *et al.* Language Models are Few-shot Learners. In Advances in Neural Information Processing Systems, 1877-1901 (2020).
- [7] Goodfellow, I. *et al.* Generative adversarial networks. Communications of the ACM, 63(11), 139-144 (2020).
- [8] Kingma, D. P., & Welling, M. Auto-encoding variational bayes. Preprint at <https://arxiv.org/abs/1312.6114> (2014).
- [9] Ho, J., Jain, A., & Abbeel, P. Denoising diffusion probabilistic models. In Advances in Neural Information Processing Systems, 33, 6840-6851 (2020).
- [10] Antol, S., Agrawal, A., Lu, J., Mitchell, M., Batra, D., Zitnick, C. L., & Parikh, D. VQA: Visual question answering. In IEEE International Conference on Computer Vision, 2425-2433 (2015).
- [11] Johnson, J., Hariharan, B., Van Der Maaten, L., Fei-Fei, L., Lawrence Zitnick, C., & Girshick, R. Girshick. CLEVR: A Diagnostic Dataset for Compositional Language and Elementary Visual Reasoning. In IEEE Conference on Computer Vision and Pattern Recognition, 2901-2910 (2017).
- [12] Wang, X., Wei, J., Schuurmans, D., Le, Q., Chi, E., & Zhou, D. Self-Consistency Improves Chain of Thought Reasoning in Language Models. Preprint at <https://arxiv.org/abs/2203.11171> (2022).
- [13] Drori, I. *et al.* A Neural Network Solves, Explains, and Generates University Math Problems by Program Synthesis and Few-shot Learning at Human Level. Proceedings of the National Academy of Sciences, 119 (2022).
- [14] Chen, M. *et al.* Evaluating Large Language Models Trained on Code. Preprint at <https://arxiv.org/abs/2107.03374> (2021).
- [15] Depeweg, S., Rothkopf, C. A., & Jäkel, F. Solving Bongard Problems with a Visual Language and Pragmatic Reasoning. Preprint at <https://arxiv.org/abs/1804.04452> (2018).
- [16] Nie, W., Yu, Z., Mao, L., Patel, A. B., Zhu, Y., & Anandkumar, A. Bongard-LOGO: A New Benchmark for Human-Level Concept Learning and Reasoning. In Advances in Neural Information Processing Systems, 16468–16480 (2020).
- [17] Raven J. C. Raven’s Progressive Matrices. (Western Psychological Services, (1938).
- [18] Dosovitskiy, A. *et al.* An Image is Worth 16x16 Words: Transformers for Image Recognition at Scale. Preprint at <https://arxiv.org/abs/2010.11929> (2020).
- [19] Zhang, C., Gao, F., Jia, B., Zhu, Y., & Zhu, S. C. Raven: A Dataset for Relational and Analogical Visual Reasoning. In Proceedings of the IEEE/CVF Conference on Computer Vision and Pattern Recognition, 5317–5327 (2019).
- [20] Barrett, D., Hill, F., Santoro, A., Morcos, A., & Lillicrap, T. Measuring Abstract Reasoning in Neural Networks. In International Conference on Machine Learning, 511–520 (2018).
- [21] Zheng, K., Zha, Z. J., & Wei, W. Abstract Reasoning with Distracting Features. In Advances in Neural Information Processing Systems, (2019).
- [22] Zhang, C., Jia, B., Gao, F., Zhu, Y., Lu, H., & Zhu, S. C. Learning Perceptual Inference by Contrasting. In Proceedings of Advances in Neural Information Processing Systems, (2019).
- [23] Zhuo, T., & Kankanhalli, M. Effective Abstract Reasoning with Dual-Contrast Network. In Proceedings of International Conference on Learning Representations, (2020).
- [24] Benny, Y., Pekar, N., & Wolf, L. Scale-Localized Abstract Reasoning. In Proceedings of the IEEE/CVF Conference on Computer Vision and Pattern Recognition, 12557-12565, (2021).
- [25] Wu, Y., Dong, H., Grosse, R., & Ba, J. The Scattering Compositional Learner: Discovering Objects, Attributes, Relationships in Analogical Reasoning. Preprint at <https://arxiv.org/abs/2007.04212> (2020).
- [26] Sahu, P., Basioti, K., & Pavlovic, V. SAViR-T: Spatially Attentive Visual Reasoning with Transformers. Preprint at <https://arxiv.org/abs/2206.09265> (2022).
- [27] Van Steenkiste, S., Locatello, F., Schmidhuber, J., & Bachem, O. Are Disentangled Representations Helpful for Abstract Visual Reasoning? In Advances in Neural Information Processing Systems, (2019)
- [28] Zhang, C., Jia, B., Zhu, S. C., & Zhu, Y. Abstract Spatial-Temporal Reasoning via Probabilistic Abduction and Execution. In Proceedings of the IEEE/CVF Conference on Computer Vision and Pattern Recognition, 9736-9746 (2021).
- [29] Zhang, C., Xie, S., Jia, B., Wu, Y. N., Zhu, S. C., & Zhu, Y. Learning Algebraic Representation for Systematic Generalization. In Proceedings of the European Conference on Computer Vision, (2022).

- [30] Hersche, M., Zeqiri, M., Benini, L., Sebastian, A., & Rahimi, A. A Neuro-vector-symbolic Architecture for Solving Raven’s Progressive Matrices. Preprint at <https://arxiv.org/abs/2203.04571> (2022).
- [31] Hu, S., Ma, Y., Liu, X., Wei, Y., & Bai, S. Stratified Rule-Aware Network for Abstract Visual Reasoning. In Proceedings of the AAAI Conference on Artificial Intelligence, 1567-1574 (2021).
- [32] Zhuo, T., Huang, Q., & Kankanhalli, M. Unsupervised Abstract Reasoning for Raven’s Problem Matrices. IEEE Transactions on Image Processing, 8332 - 8341 (2021).
- [33] Carpenter, P. A., Just, M. A., & Shell, P. What One Intelligence Test Measures: a Theoretical Account of the Processing in the Raven Progressive Matrices Test. Psychological review, 97(3), 404, (1990).
- [34] Chen, T., Kornblith, S., Norouzi, M., & Hinton, G. A Simple Framework for Contrastive Learning of Visual Representations. In Proceedings of the International Conference on Machine Learning, 1597–1607 (2020).
- [35] Oord, A. V. D., Li, Y., & Vinyals, O. Representation Learning with Contrastive Predictive Coding. Preprint at <https://arxiv.org/abs/1807.03748> (2019).
- [36] He, K., Fan, H., Wu, Y., Xie, S., & Girshick, R. Momentum Contrast for Unsupervised Visual Representation Learning. In Proceedings of the IEEE/CVF Conference on Computer Vision and Pattern Recognition, 9729-9738 (2020).
- [37] Gehring, J., Auli, M., Grangier, D., Yarats, D., & Dauphin, Y. N. Convolutional Sequence to Sequence Learning. In Proceedings of the International Conference on Machine Learning, 1243–1252 (2017).
- [38] Paszke, A. *et al.* Automatic Differentiation in Pytorch. In NIPS Autodiff Workshop, (2017).
- [39] Kingma, D. P., & Ba, J. Adam: A Method for Stochastic Optimization. Preprint at <https://arxiv.org/abs/1412.6980>, (2014).
- [40] Sun, C., Shrivastava, A., Singh, S., & Gupta, A. Revisiting Unreasonable Effectiveness of Data in Deep Learning Era. In Proceedings of the IEEE International Conference on Computer Vision, 843-852, (2017).
- [41] Cordonnier, J. B., Loukas, A., & Jaggi, M. On the Relationship between Self-Attention and Convolutional Layers. In Proceedings of International Conference on Learning Representations, (2020).
- [42] Wang, H. *et al.* Score-CAM: Score-Weighted Visual Explanations for Convolutional Neural Networks. In Proceedings of the IEEE/CVF Conference on Computer Vision and Pattern Recognition Workshops, (2020).
- [43] Petsiuk, V., Das, A., & Saenko, K. Rise: Randomized Input Sampling for Explanation of Black-box Models. Preprint at <https://arxiv.org/abs/1806.07421> (2018).